EJN European Journal of Neuroscience

FENS Federation of European Neuroscience Societies

European Journal of Neuroscience, Vol. 45, pp. 299–311, 2017 doi:10.1111/ejn.13463

COGNITIVE NEUROSCIENCE

Ageing affects dual encoding of periodicity and envelope shape in rat inferior colliculus neurons

Björn Herrmann,[1] Aravindakshan Parthasarathy[2,3,4] and Edward L. Bartlett[2]
[1]Department of Psychology & Brain and Mind Institute, The University of Western Ontario, London, ON, N6A 3K7, Canada
[2]Departments of Biological Sciences and Biomedical Engineering, Purdue University, West Lafayette, IN, USA
[3]Department of Otology and Laryngology, Harvard Medical School, Boston, MA, USA
[4]Eaton-Peabody Laboratories, Massachusetts Eye and Ear Infirmary, Boston, MA, USA

Keywords: ageing, amplitude modulation, inferior colliculus, neural synchronisation, rats

Edited by John Foxe
Received 26 June 2016, revised 19 October 2016, accepted 31 October 2016

Abstract

Extracting temporal periodicities and envelope shapes of sounds is important for listening within complex auditory scenes but declines behaviorally with age. Here, we recorded local field potentials (LFPs) and spikes to investigate how ageing affects the neural representations of different modulation rates and envelope shapes in the inferior colliculus of rats. We specifically aimed to explore the input–output (LFP-spike) response transformations of inferior colliculus neurons. Our results show that envelope shapes up to 256-Hz modulation rates are represented in the neural synchronisation phase lags in younger and older animals. Critically, ageing was associated with (i) an enhanced gain in onset response magnitude from LFPs to spikes; (ii) an enhanced gain in neural synchronisation strength from LFPs to spikes for a low modulation rate (45 Hz); (iii) a decrease in LFP synchronisation strength for higher modulation rates (128 and 256 Hz) and (iv) changes in neural synchronisation strength to different envelope shapes. The current age-related changes are discussed in the context of an altered excitation-inhibition balance accompanying ageing.

Introduction

Natural environmental sounds such as speech or music vary on multiple time scales. The temporal structure of sounds – for example, the rate of an amplitude modulation (AM) or the shape of an amplitude envelope – is a crucial acoustic feature on which basis different sounds are perceptually distinguishable (Patterson, 1994; Akeroyd & Patterson, 1995; Irino & Patterson, 1996; Furukawa & Moore, 1997). Neurophysiological studies in humans and animals show that neural activity synchronises with a sound's amplitude modulation likely supporting perceptual discriminability (Picton *et al.*, 2003; Joris *et al.*, 2004). Neural synchronisation has been observed at all stages of the auditory system ranging from auditory nerve fibres to auditory cortex (Vernier & Galambos, 1957; Epping & Eggermont, 1986; Preuß & Müller-Preuss, 1990; Joris & Yin, 1992; Palombi *et al.*, 2001; Bibikov, 2002; Joris *et al.*, 2004; Bartlett & Wang, 2005, 2007, 2011; Malone *et al.*, 2007; Kadner & Berrebi, 2008; Kale & Heinz, 2010; Herrmann *et al.*, 2013a; Parthasarathy *et al.*, 2014). Furthermore, neural synchronisation is influenced by the rate of the temporal modulation and the envelope shape of the modulation (Pressnitzer *et al.*, 2000; Lu *et al.*, 2001; Neuert *et al.*, 2001; Parthasarathy & Bartlett, 2011).

Correspondence: B. Herrmann, as above.
E-mail: herrmann.b@gmail.com

Critically, hearing abilities, including perception of temporal aspects of sounds, decline with ageing and hearing loss (Barsz *et al.*, 2002; Pichora-Fuller, 2003; Walton, 2010). For example, gap detection as well as detection of temporal modulation is impaired in older listeners (Schneider *et al.*, 1994; Moore & Skrodzka, 2002). Hearing difficulties in ageing might be related to sensory degradation, alterations of the central auditory system, and/or cognitive decline (Canlon *et al.*, 2010; Wayne & Johnsrude, 2015). In particular alterations of the central auditory system due to ageing or hearing loss can be drastic, including reduced neuronal inhibition (Caspary *et al.*, 1995; Burianova *et al.*, 2009; Llano *et al.*, 2012; Rabang *et al.*, 2012; Takesian *et al.*, 2012; for a review see Caspary *et al.*, 2008) and increased neuronal responses (Popelár *et al.*, 1987; Syka *et al.*, 1994; Hughes *et al.*, 2010; Manzoor *et al.*, 2012; Stolzberg *et al.*, 2012) along the auditory pathway. Furthermore, neural synchronisation in aged animals appears to be enhanced for lower modulation rates but reduced for fast modulation rates (Palombi *et al.*, 2001; Schatteman *et al.*, 2008; for compatible work in humans see Purcell *et al.*, 2004; Bidelman *et al.*, 2014). Population responses (likely originating from the brainstem and midbrain) indicate age-related deficits in envelope-shape coding (Parthasarathy & Bartlett, 2011) and also suggest central gain enhancement of responses with ageing (Parthasarathy *et al.*, 2014).

Extracellular neuronal signals are commonly separated into spiking activity and slower potential fluctuations referred to as local field

potentials (LFPs). Previous studies on sensory representations have focused on spiking activity (e.g. Palombi *et al.*, 2001; Schatteman *et al.*, 2008; Bartlett & Wang, 2011). More recently, the importance of field potentials in sensation has been emphasised (e.g. Lakatos *et al.*, 2008; Whittingstall & Logothetis, 2009; Belitski *et al.*, 2010; Haegens *et al.*, 2011; Kajikawa & Schroeder, 2011; Kayser *et al.*, 2015), but the extracellular LFP has remained largely unexplored in the study of ageing animals (but see Gourévitch & Edeline, 2011). Yet, spiking activity primarily reflects the output of a neuron or neuronal population, whereas the LFP largely reflects the synaptic activity at the dendrites and soma, and thus contains information about the aggregate input to a neuron or neuronal population (but other non-synaptic activity might additionally contribute; Bullock, 1997; Logothetis *et al.*, 2001; Logothetis & Wandell, 2004; Buzsáki *et al.*, 2012). While the age- and hearing loss-related augmentation of neural firing along the ascending auditory pathway is well established (using neuronal spiking; Popelár *et al.*, 1987; Hughes *et al.*, 2010), the relative change from synaptic (input) activity to neuronal spiking output within a single brain structure and the age-related changes thereof are unknown. In particular, the inferior colliculus in the midbrain is a prime candidate in which age-related changes in sensory transformation might occur due to the inferior colliculus' relevance in integrating ascending sensory and descending neural signals (Adams, 1979; Pollak *et al.*, 2003; Lee & Sherman, 2010) along with the age-related reduction in neural inhibition (Milbrandt *et al.*, 1994; Raza *et al.*, 1994; Caspary *et al.*, 1995; Burianova *et al.*, 2009; Rabang *et al.*, 2012).

This study investigates neuronal activity of inferior colliculus neurons in younger and older rats in response to amplitude-modulated sounds, varying in modulation rate and envelope shape. We specifically aimed to investigate whether ageing affects the sensory transformation from synaptic neuronal signals (LFP) to spiking activity. Our main findings were (i) that onset-evoked LFPs were smaller for older compared to younger rats, whereas there was no difference in onset-evoked spiking activity; (ii) that neural synchronisation strength of LFPs was similar between age groups, whereas spike synchronisation was increased for older rats at a low modulation rate; (iii) that neural synchronisation for fast modulation rates was larger for younger compared to older animals. We also observed age-related differences in neural synchronisation specifically related to the envelope shape.

Methods and materials

Ethical approval

The experimental procedures described in the present investigation were approved by the Institutional Animal Care and Use Committee of Purdue University (PACUC #1111000167). The experiments included in this study comply with the policies and regulations described by Drummond (2009). Rats were housed one per cage in accredited facilities (Association for the Assessment and Accreditation of Laboratory Animal Care) with food and water provided *ad libitum*. The number of animals used was reduced to the minimum necessary to allow adequate statistical analyses.

Surgical procedures

Nine young (3–6 months, ~300 g) and eleven older (22–26 months, ~400–500 g) male Fischer-344 rats were used in this study. The ageing Fisher-344 rat has been suggested to be a suitable model to study presbycusis in ageing animals (Syka, 2010). Many of the animals in the study were tested for hearing threshold using the auditory brainstem response (ABR). The ABR responses showed clear age-related changes in hearing thresholds (all values dB SPL and standard deviation: nine older animals: click 53.3 ± 6.6, 8 kHz tone 36.7 ± 2.5; nine younger animals: click 36.4 ± 3.8, 8 kHz tone 30.0 ± 7.5), with a larger threshold discrepancy for clicks vs. 8 kHz tones as reported previously (Parthasarathy & Bartlett, 2011). Methods for surgery, sound stimulation and recording are similar to those described in (Rabang *et al.*, 2012; Herrmann *et al.*, 2015). Surgeries and recordings were performed in a 9′ × 9′ double walled acoustic chamber (Industrial Acoustics Corporation). Animals were anaesthetised using a mixture of ketamine (VetaKet, 80 mg/kg) and dexmedetomidine (Dexdomitor, 0.2 mg/kg) administered intra-muscularly via injection. A constant physiological body temperature was maintained using a water-circulated heating pad (Gaymar) set at 37 °C with the pump placed outside the recording chamber to eliminate audio and electrical interferences. The animals were maintained on oxygen through a manifold. The pulse rate and oxygen saturation were monitored using a pulse-oximeter to ensure they were within normal ranges during surgery. Supplementary doses of anaesthesia (20 mg/kg of ketamine, 0.05 mg/kg of dexmedetomidine) were administered intra-muscularly as required to maintain areflexia and a surgical plane of anaesthesia. An initial dose of dexamethasone and atropine was administered prior to incision to reduce swelling and mucosal secretions. A subdermal injection of Lidocaine (0.5 mL) was administered at the site prior to first incision. A central incision was made along the midline, and the calvaria exposed. A stainless steel headpost was secured anterior to bregma using an adhesive and three screws drilled into the skull to provide structural support for a head-cap, constructed of orthodontic resin (Dentsply). A craniotomy was performed from 9 to 13 mm posterior to bregma, which extended posterior to the lambda suture, and 3 mm wide extending from the midline. The dura mater was kept intact, and the site of recording was estimated stereotaxically using a rat atlas (Paxinos & Watson, 2006) as well as using internal vasculature landmarks and physiological measurements. At the completion of recordings, animals were euthanised with Beuthanasia (200 mg/kg IP). Once areflexive, they were perfused transcardially with 150–200 mL phosphate buffered saline followed by 400–500 mL 4% paraformaldehyde. The brain was then removed and stored or processed further for Nissl or immunohistochemistry.

Stimulus generation

Sound stimuli were generated using SigGenRP (Tucker-Davis Technologies, TDT) at a 97.64 kHz sampling rate (standard TDT sampling rate) and presented through custom-written interfaces in OPENEX software (TDT). Sound waveforms were generated via a multichannel processor (RX6, TDT), amplified (SA1, TDT), and presented free-field through a Bowers and Wilkins DM601 speaker. The sounds were presented to the animal at azimuth 0° and elevation 0°, calibrated at a distance of 115 cm from speaker to ear, using a Bruel & Kjaer microphone and SIGCAL software (TDT). All recordings took place in an Industrial Acoustics booth lined with 1 inch (35 mm) Sonex foam with ~90% absorption for frequencies ≥1000 Hz, minimising potential echoes or reverberations.

Acoustic stimulation

Stimuli consisted of white noise carriers that were modulated in amplitude at three different modulation rates using five different envelope shapes. Modulation rates were 45, 128 and 256 Hz

(Fig. 1, left). These rates were chosen to be comparable to our previous studies (Parthasarathy & Bartlett, 2011; Parthasarathy *et al.*, 2014) and to test the limits of temporal precision, rather than testing slower amplitude-modulation rates. This set of modulation frequencies is also in accordance with human studies investigating age-related changes in neural synchronisation to amplitude-modulated sounds (Boettcher *et al.*, 2001; Purcell *et al.*, 2004; Grose *et al.*, 2009). The modulation frequencies in our study, though not dominant in terms of stimulus energy, are also critical for proper gender identification and are affected by ageing (Schvartz & Chatterjee, 2012).

Envelope shapes ranged from strongly damped to strongly ramped generated by varying parameters of a beta function (Fig. 1, middle). The beta function for one cycle ($\boldsymbol{b}$) was defined as follows:

$$\boldsymbol{b} = \boldsymbol{t}^{z-1}(1-\boldsymbol{t})$$

where $\boldsymbol{t}$ is a time vector ranging from 0 to 1 (covering a full cycle duration) and z the parameter determining the envelope shape. The parameter z could take on one of three values: 1.05, 1.4491 or 2; relating to strongly damped, weakly damped and symmetrical envelopes respectively. For the weakly and strongly ramped envelope shapes the beta functions generated for z values of 1.4491 and 1.05 were time-reversed respectively (Fig. 1, middle). Beta functions were peak-normalised. Sounds had duration of approximately ~265 ms depending on modulation frequency, and sounds were presented every 1.25 s. Each of the 3 × 5 (modulation rate × envelope shape) sounds was randomly presented between 6 and 10 times (typically 10 times; consistent number within a unit).

Electrophysiological recordings

Single unit activity and multiunit activity in the inferior colliculus was recorded *in vivo* using a tungsten microelectrode (A-M Systems) encased in a glass capillary that was advanced using a hydraulic micro-drive (Narishige). We recorded 93 units in younger rats and 90 units in older rats. The inferior colliculus was identified based on short-latency driven responses to tone stimuli. The central nucleus of the inferior colliculus was identified using the ascending tonotopy moving in a dorsoventral direction as well as narrowly tuned responses to pure tones with frequencies ranging from 0.5 to 40 kHz. Recordings were obtained from both the dorsal cortex and central nucleus. Although we cannot exclude that we recorded from lateral (or external) cortex, based on the recording depth, the presence of sustained responses to tones and amplitude-modulated stimuli, as well as clear frequency tuning in most cases, we estimate that most of our units were recorded from the central nucleus.

Neural signals were acquired using the tungsten microelectrode connected to a headstage (RA4, TDT) and were amplified (RA4PA preamplifier, TDT). The digitised waveforms and spike times were recorded with a multichannel recording and stimulation system (RZ-5, TDT) at a sampling rate of 24.41 kHz (standard TDT sampling rate). The interface for acquisition and spike sorting were custom made using the OPENEX and RPVDSEX software (TDT). The units acquired were filtered between 500 Hz (occasionally 300 Hz) and 5000 Hz. The acquired spikes were stored in a data tank and analysed using custom written software in MATLAB. Local field potentials were simultaneously recorded from the same electrode by sampling at 1525.88 Hz and bandpass filtering from 3 to 500 Hz. Line noise at 60 Hz was offline removed from the local field potential recordings using an elliptic notch filtre (infinite-impulse response; zero-phase lag).

Data analysis: onset and sustained responses

All offline data analyses were carried out in MATLAB (MathWorks Inc.). Response time courses were calculated for visualisation purposes as the average across single-trial time courses (LFP) or peri-stimulus time histograms (spikes; 0.5 ms time steps, 4 ms moving rectangular window). Response magnitudes were assessed for an onset and a sustained time window. The onset time window ranged from 0 to 0.05 s and the sustained time window ranged from 0.05 to 0.275 s. For spikes, firing rates were calculated. For local field potentials, the response magnitude was calculated as the root-mean-squared amplitude.

Onset response latencies for the LFPs were extracted for the N1 (negative peak within 0–0.05 s). P1 latencies were not analysed to avoid unreliable estimates for older rats. The latency of the first spike was extracted for trials eliciting at least one spike within the 0–0.05 s time window after stimulus onset (Heil, 2004).

Data analysis: neural synchronisation to amplitude-modulated sounds

Neural synchronisation for local field potentials was calculated as follows. For each modulation rate and envelope shape condition

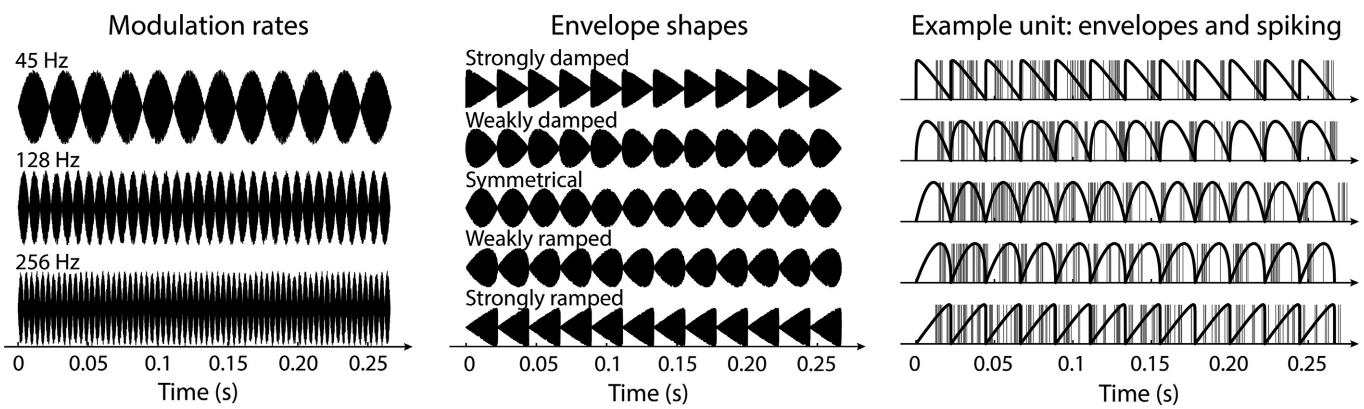

FIG. 1. Stimulation conditions and example unit. Left: rats were stimulated with three different modulation rates: 45, 128 and 256 Hz (here the symmetrical envelope shape is displayed). Middle: amplitude-modulated noise carrier. Five different envelope shapes ranging from strongly damped to strongly ramped amplitude modulations (with a 45-Hz modulation rate in the example). Right: spiking responses of an example unit to different envelope shapes for a 45-Hz modulation rate. Envelopes are plotted in black solid lines. Gray vertical lines reflect spikes.

separately, single-trial time courses were averaged, the 0.05–0.275 s time interval was extracted, and a fast Fourier transform (FFT) was calculated (zero-padding to obtain a frequency resolution of 0.25 Hz; 20–300 Hz). An amplitude spectrum and a phase spectrum was calculated as the magnitude and the angle, respectively, of the FFT complex values. Neural synchronisation strength at the AM frequency was quantified as the mean amplitude across a 2-Hz frequency window centred on the AM frequency. The mean phase angle at the AM frequency, reflecting the phase delay/lag, was quantified as the circular mean across a 2-Hz frequency window centred on the AM frequency.

Neural synchronisation for spiking activity was calculated as follows. For each modulation rate and envelope shape condition separately, spikes times were extracted from the 0.05 to 0.275 s time interval. Spike times were transformed to phase angles ($\boldsymbol{p}$) using the following formula:

$$\boldsymbol{p} = -2f\boldsymbol{t}\pi + \pi,$$

where f is frequency and $\boldsymbol{t}$ a vector of spike times (of all trials of one condition). The minus sign in combination with the added π ensured that spiking phase angles and local field potential phase angles were comparable. Phase angles were wrapped to range from $-\pi$ to π. Using the spikes of all trials of one condition, the empirical vector strength v, that is, the resultant vector length, was calculated as follows (Lachaux *et al.*, 1999):

$$\boldsymbol{v} = \frac{1}{n}\left|\sum_{j=1}^{n} e^{i\boldsymbol{p}_j}\right|,$$

where $\boldsymbol{v}$ is the vector strength, i the imaginary unit, $\boldsymbol{p}$ the vector of phase angles, and n the number of spikes (with j being the index). The vector strength can be biased by the number of spikes, with smaller v values for a higher number of spikes. For that reason, a normalised vector strength was calculated. To this end, n (number of spikes of a condition) random phase values between $-\pi$ and π were generated and the vector strength (i.e. the resultant vector length) was calculated. Randomly drawing phase values and calculation of the vector strength was repeated 5000 times, which resulted in a distribution of random vector strengths given the number of spikes. The normalised vector strength was then calculated by subtracting the empirical vector strength from the mean of the random vector strength distribution and dividing the result by the standard deviation of the random vector strength distribution. The normalised vector strength was calculated for frequencies (f) ranging from 20 to 300 Hz with a frequency resolution of 1 Hz, resulting in a vector strength spectrum. A phase spectrum was calculated as the circular mean across single-spike phase values ($\boldsymbol{p}$) for each frequency. Neural synchronisation strength at the AM frequency was quantified as the mean normalised vector strength across a 2-Hz frequency window centred on the AM frequency. The mean phase angle at the AM frequency, reflecting the phase delay, was quantified as the circular mean across a 2-Hz frequency window centred on the AM frequency.

We also calculated the percentage of units that could be considered highly sensitive to the specific modulation rates. For spikes synchronisation, the normalised vector strength reflects a statistical measure – a z-score – and we considered a unit to be sensitive to a modulation rate if its normalised vector strength was equal or larger than 1.645 (i.e. one-tailed $P \leq 0.05$). For LFP synchronisation, a $1/f$ pattern was observed for the amplitude spectra (Fig. 4) requiring a different approach for the LFPs. Here, we made use of a 95% confidence interval (i.e. one-tailed $P \leq 0.05$; Gardner & Altman, 1986). In detail, the confidence interval for a given stimulus modulation rate was calculated by making use of the amplitudes of the other two stimulus modulation rates. For example, the confidence interval for the 45-Hz modulation rate condition was calculated using the amplitudes at 45 Hz of the 128- and 256-Hz modulation rate conditions (for 128 Hz the 45- and 256-Hz modulation rates were used; for 256 Hz only the 45-Hz modulation rate was used because 128 Hz produced a harmonic response at 256 Hz). Finally, we considered a unit to be sensitive to a modulation rate if its amplitude at the modulation frequency was equal or greater than the respective 95% confidence interval.

Statistical analyses

For the statistical analyses, we utilised the Wilcoxon rank-sum test to compare different age groups and the Wilcoxon signed rank test for within-unit (repeated-measures) comparisons using the Matlab inbuilt functions (ranksum, signrank; respectively). Effect sizes are reported as $r_{\text{equivalent}}$ (Rosenthal & Rubin, 2003; hereafter referred to simply as r) for statistical tests of linear dependent measures. $r_{\text{equivalent}}$ is equivalent to a Pearson product-moment correlation for two continuous variables, to a point-biserial correlation for one continuous and one dichotomous variable, and to the square root of partial η^2 (eta-squared) for ANOVAs. Where appropriate, false discovery rate (FDR) was applied to control the proportion of false positives among significant comparisons (Benjamini & Hochberg, 1995; Genovese *et al.*, 2002).

Results

Response magnitudes of local field potential and spiking activity

First, we investigated responses to the onset of sounds independent of envelope shape, focusing on the 0–0.05 s time interval. For the local field potentials, responses were significantly larger for younger compared to older rats for all three modulation rates (root-mean-squared amplitudes; 45 Hz: $P_{\text{FDR}} = 0.001$, $r = 0.401$; 128 Hz: $P_{\text{FDR}} < 0.001$, $r = 0.419$; 256 Hz: $P_{\text{FDR}} < 0.001$, $r = 0.412$; Fig. 2A). In contrast, firing rates were not different between age groups (45 Hz: $P_{\text{FDR}} > 0.05$, $r = 0.010$; 128 Hz: $P_{\text{FDR}} > 0.05$, $r = 0.044$; 256 Hz: $P_{\text{FDR}} > 0.05$, $r = 0.073$; Fig. 2B). Firing rates were additionally examined for the sustained time interval ranging from 0.05 to 0.275 s. Again, no significant difference between age groups was observed (45 Hz: $P_{\text{FDR}} > 0.05$, $r = 0.015$; 128 Hz: $P_{\text{FDR}} > 0.05$, $r = 0.094$; 256 Hz: $P_{\text{FDR}} > 0.05$, $r = 0.146$; Fig. 2B).

To directly compare whether ageing affects the response-magnitude relationship between local field potentials and spikes, we calculated for each unit the ratio between the root-mean-squared local field potential amplitude and the firing rates for the two time windows of interest. For the onset time window (0–0.05 s), the ratio was significantly smaller for older compared to younger rats for all three modulation rates (45 Hz: $P_{\text{FDR}} < 0.01$, $r = 0.227$; 128 Hz: $P_{\text{FDR}} = 0.01$, $r = 0.219$; 256 Hz: $P_{\text{FDR}} = 0.05$, $r = 0.179$), suggesting that a relatively smaller synaptic (input) activity is sufficient to elicit spiking (output) activity in older rats. No difference between age groups was found for the sustained time window (0.05–0.275 s; for all $P_{\text{FDR}} > 0.05$, $r < 0.13$). An analysis contrasting firing rates for damped vs. ramped envelopes is provided in the Supporting Information Fig. S1.

Response latencies of local field potential and spiking activity

Figure 3 shows responses latencies for local field potentials and spikes. Median N1 latencies were significantly smaller for older than younger rats (45 Hz: $P_{FDR} < 0.01$, $r = 0.318$; 128 Hz: $P_{FDR} = 0.01$, $r = 0.306$; 256 Hz: $P_{FDR} < 0.01$, $r = 0.322$). In addition, N1 latencies were smaller for damped compared to ramped envelope shapes (collapsed across weakly and strongly damped/ramped) for the 45-Hz modulation rate (younger: $P_{FDR} = 0.05$, $r = 0.240$; older: $P_{FDR} < 0.05$, $r = 0.299$; no age group difference: $P_{FDR} > 0.05$, $r = 0.088$). There was no difference in N1 latencies between damped and ramped envelope shapes for the 128-Hz and the 256-Hz modulation rate (for all, $P_{FDR} > 0.05$, $r < 0.25$).

The median latencies of the first spike did not differ between age groups (45 Hz: $P_{FDR} > 0.05$, $r = 0.080$; 128 Hz: $P_{FDR} > 0.05$, $r = 0.061$; 256 Hz: $P_{FDR} > 0.05$, $r = 0.028$). The spike latencies were smaller for damped compared to ramped envelope shapes (collapsed across weakly and strongly damped/ramped) for the 45-Hz modulation rate (younger: $P_{FDR} < 0.05$, $r = 0.465$; older: $P_{FDR} < 0.05$, $r = 0.474$; no age group difference: $P_{FDR} > 0.05$, $r = 0.094$) and for younger rats for the 256-Hz modulation rate (younger: $P_{FDR} < 0.05$, $r = 0.369$; older: $P_{FDR} > 0.05$, $r = 0.065$; and a larger increase for younger rats: $P_{FDR} = 0.05$, $r = 0.234$). There were no effects of latency as a function of envelope shape for the 128-Hz modulation rate (for all, $P_{FDR} > 0.05$, $r < 0.10$).

Neural synchronisation strength of local field potentials and spiking activity

Figure 4 shows neural synchronisation strength of local field potentials and spiking activity. We observed clear peaks in the LFP amplitude spectrum at each AM frequency. Similarly, clear peaks were observed for spike synchronisation at the AM frequencies.

For local field potentials, synchronisation strength at the AM frequency was significantly larger for younger compared to older rats for 128 Hz ($P_{FDR} = 0.001$, $r = 0.300$) and 256 Hz ($P_{FDR} = 0.01$, $r = 0.236$), whereas there was no difference between age groups at 45 Hz ($P_{FDR} > 0.10$, $r = 0.010$; Fig. 4). For spiking activity, synchronisation strength at the AM frequency was significantly larger for older compared to younger rats for 45 Hz ($P_{FDR} < 0.01$, $r = 0.262$). No difference between age groups was observed for 128 Hz ($P_{FDR} > 0.05$, $r = 0.022$; Fig. 4) and 256 Hz ($P_{FDR} > 0.05$, $r = 0.160$, although the effect was significant for an uncorrected P-value). The percentages of modulation-rate sensitive neurons are provided in the small insets in Fig. 4. In sum, neural synchronisation in older rats was systematically reduced (compared to younger rats) for fast modulation rates (although not statistically significant in some cases). In contrast, spike synchronisation to the low modulation rate (45 Hz) was enhanced for older animals.

Figure 5 further displays the age difference in neural synchronisation for the 45-Hz modulation rate using inter-spike-intervals. That is, for each trial with two or more spikes within the 0.05–0.275 s

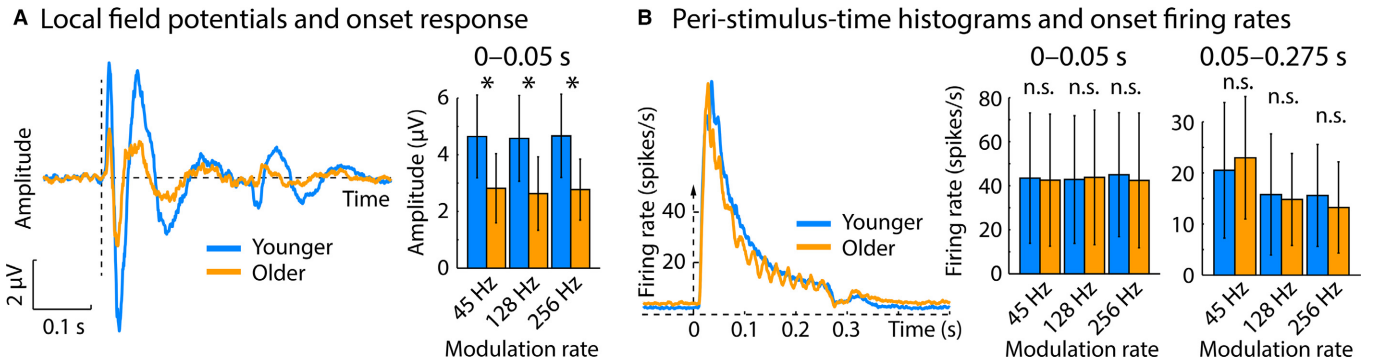

FIG. 2. Response magnitude of local field potentials and spiking activity. (A) Time courses of local field potentials averaged across all conditions (modulation rate; envelope shape). The late bump for young rats is due to the stimulus offset. Bar graphs show median root-mean-squared amplitudes (0–0.05 s). Error bars reflect the semi-interquartile range. (B) Peri-stimulus-time histograms (across all conditions). Bar graphs show median firing rates (0–0.05 s; 0.05–0.275 s) and error bars reflect the semi-interquartile range. *$P_{FDR} < 0.05$, n.s., not significant. [Colour figure can be viewed at wileyonlinelibrary.com].

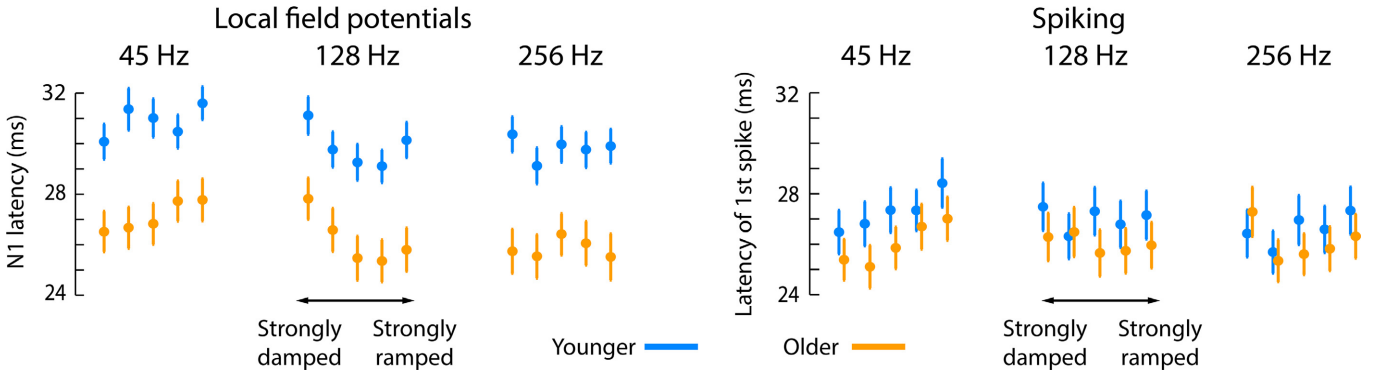

FIG. 3. Condition-specific onset latencies for N1 and first spike. Circles reflect the mean across units. The error bar reflects the standard error or the mean. [Colour figure can be viewed at wileyonlinelibrary.com].

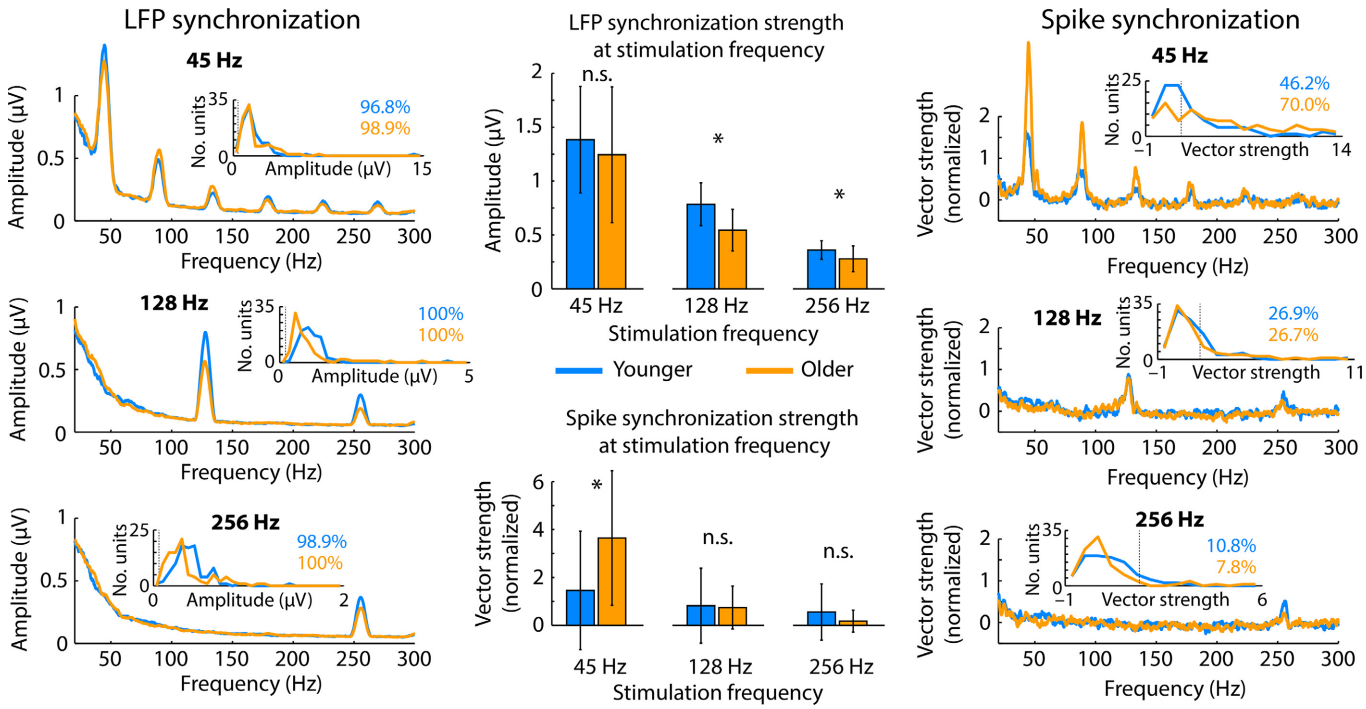

FIG. 4. Neural synchronisation of local field potentials (left) and spikes (right) for each modulation rate and age group. Small insets show unit-histograms for synchronisation strength and percentage of modulation-rate sensitive units. The thin dashed lines in the histograms indicate the significance criterion [averaged across age groups for local field potentials (LFPs)]. Bar graphs (middle) show median neural synchronisation strength. Error bars reflect the semi-interquartile range. *$P_{FDR} \leq 0.05$, n.s., not significant. [Colour figure can be viewed at wileyonlinelibrary.com].

time interval, the inter-spike-intervals were calculated. Subsequently, the relative number of inter-spike-intervals was calculated for each unit (16 non-overlapping bins of 2-ms width). This analysis revealed an increase in the relative number of short inter-spike-intervals (~3 ms; $P_{FDR} < 0.05$, $r = 0.162$) and an increase for inter-spike intervals at around the AM frequency (45 Hz, ~22.2 ms; $P_{FDR} = 0.01$, $r = 0.217$) for older compared to younger rats. In contrast, the relative number of intermediate inter-spike-intervals was increased for younger rats (~5–9 ms; $P_{FDR} < 0.01$, $r = 0.331$; Fig. 5). We further tested whether the relative increase of ~3 ms inter-spike intervals for older rats reflects an increase relative to the 45-Hz stimulation cycle or whether it reflects a nonsynchronised increase in ~3 ms inter-spike intervals. To this end, the normalised vector strength was calculated ($f = 45$ Hz) based on the phase of the first spike of the ~3 ms inter-spike-intervals (2–4 ms bin). The normalised vector strength for ~3 ms inter-spike-intervals was larger for older compared to younger rats ($P_{FDR} = 0.05$, $r = 0.160$; Fig. 5 inset). Taken together, the data indicate that there were short bursts of spikes tightly linked to the 45-Hz AM rate for older rats, whereas spikes occurred more distributed across the 45-Hz modulation cycle for younger rats.

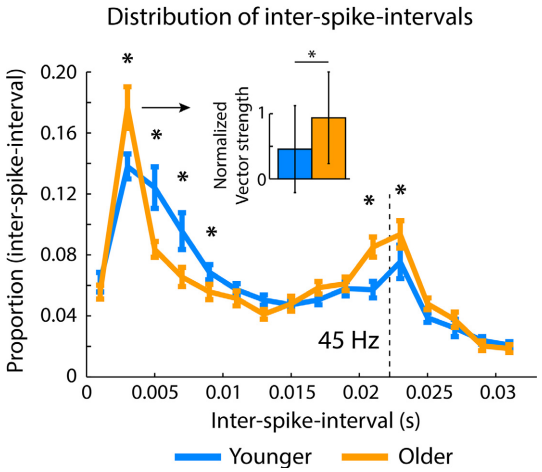

FIG. 5. Distribution of inter-spike-intervals. Distribution of inter-spike-intervals (mean across units) for the 45-Hz modulation rate stimuli. Error bars reflect the standard error of the mean. Asterisks reflect a significant difference between age groups (*$P < 0.05$). The small inset reflects the median normalised vector strength of ~3 ms inter-spike-intervals (the error bars are the semi-interquartile range), showing that the relative increase in ~3 ms inter-spike-intervals reflect tightly synchronised bursts of spikes in older rats. [Colour figure can be viewed at wileyonlinelibrary.com].

Effects of envelope shape on neural synchronisation strength

Age-related differences in neural synchronisation strength for individual envelope shapes and corresponding statistical significances are depicted in Fig. 6. To statistically assess the effect of envelope shape on neural synchronisation, we averaged the synchronisation strength for weakly and strongly damped conditions and for weakly and strongly ramped conditions. We contrasted damped vs. ramped envelope shapes independently for younger and older rats, followed by comparison of the damped-ramped difference between age groups.

The results for LFPs were as follows (Fig. 6, top row). For the 45 Hz-modulation rate, synchronisation strength was smaller for damped compared to ramped envelopes for younger rats ($P_{FDR} < 0.05$, $r = 0.254$), whereas the opposite (i.e. damped > ramped) was found for older rats ($P_{FDR} = 0.01$, $r = 0.313$). Furthermore, the damped-ramped difference was larger for older compared to younger rats ($P_{FDR} < 0.001$, $r = 0.279$). Effects for the 128-Hz modulation rate were weaker, with a stronger

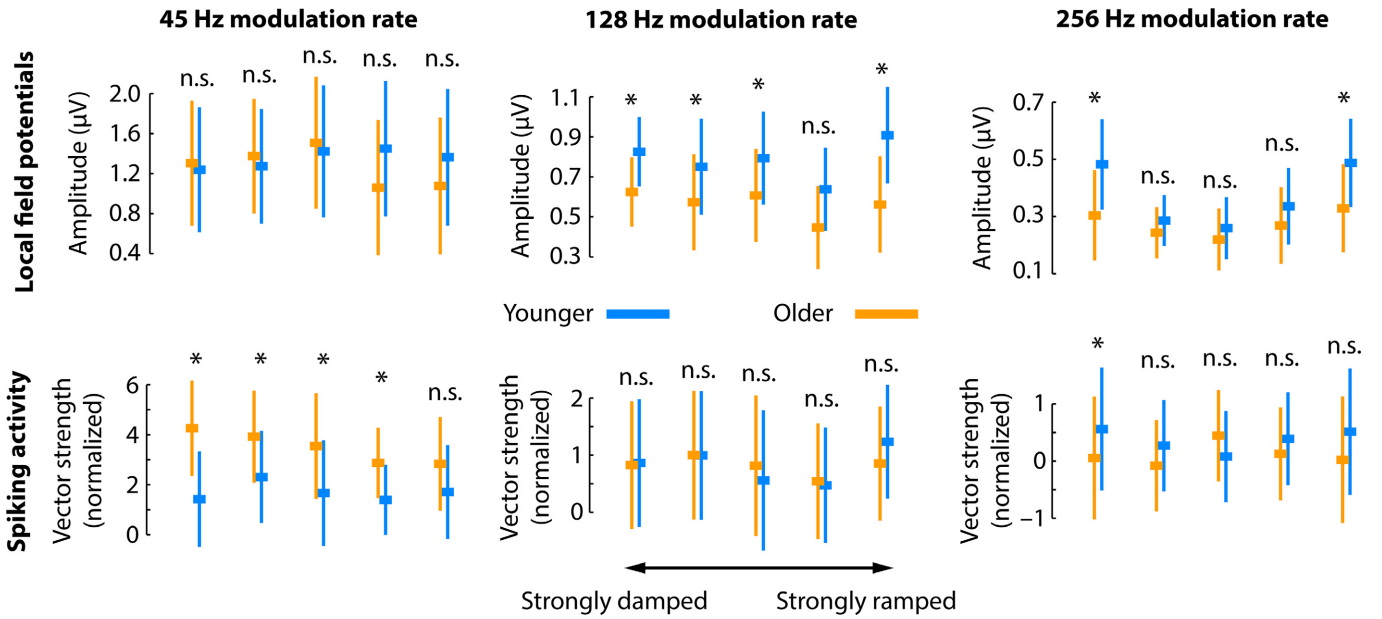

FIG. 6. Neural synchronisation strength for the three modulation-rate and five envelope-shape conditions. Top row: local field potential (LFP) synchronisation strength (amplitude). Bottom row: spike synchronisation strength (normalised vector strength). The squares reflect the median across units. The error bar is the semi-interquartile range. Statistical tests reflect the age-group comparison. *$P_{FDR} \leq 0.05$, n.s., not significant. Note that the *y*-axis is not uniform for the different modulation rates. Instead, age differences and magnitude differences as a function of envelope shape are displayed in more detail. [Colour figure can be viewed at wileyonlinelibrary.com].

synchronisation strength for damped than ramped envelopes in older rats ($P_{FDR} < 0.05$, $r = 0.292$; no effect for younger rats and no age group difference was found, for both $P_{FDR} > 0.05$, $r < 0.25$). For the 256-Hz modulation rate, there was no difference between damped and ramped envelope shapes (younger: $P_{FDR} > 0.05$, $r = 0.238$; older: $P_{FDR} > 0.05$, $r = 0.184$; age group difference: $P_{FDR} > 0.05$, $r = 0.081$). However, as depicted in Fig. 6, synchronisation strength followed a quadratic trend (younger: $P_{FDR} < 0.001$, $r = 0.678$; older: $P_{FDR} < 0.001$, $r = 0.586$) were damped as well as ramped envelopes led to strongest synchronisation. The quadratic trend was larger for younger than older rats ($P_{FDR} < 0.001$, $r = 0.338$).

The results for spike synchronisation were as follows (Fig. 6, bottom row). No effects of envelope shape were observed for the 45-Hz modulation rate when synchronisation strength was collapsed across weakly and strongly damped/ramped shapes. However, synchronisation strength for the strongly damped shape was larger than for the strongly ramped shape for older rats ($P_{FDR} < 0.05$, $r = 0.282$; younger rats: $P_{FDR} > 0.05$, $r < 0.01$), but this difference did not differ between age groups when FDR-corrected ($P_{FDR} > 0.05$, $r = 0.164$). There were no effects of envelope shape for the 128-Hz modulation rate (for all $P_{FDR} > 0.05$, $r < 0.15$). For the 256-Hz modulation rate, there was no difference between damped and ramped envelope shapes (younger: $P_{FDR} > 0.05$, $r = 0.032$; older: $P_{FDR} > 0.05$, $r = 0.044$; age group difference: $P_{FDR} > 0.05$, $r = 0.008$). However, similar to LFP synchronisation, spike synchronisation strength followed a quadratic trend for younger rats ($P_{FDR} < 0.001$, $r = 0.386$), but not for older rats ($P_{FDR} > 0.05$, $r = 0.016$), and the quadratic trend was larger for younger than older rats ($P_{FDR} < 0.01$, $r = 0.232$).

Relative phase delay differences between envelope shapes

Next we examined the relative phase delay (i.e. the phase angle) of neural synchronisation for sounds modulated by different envelope shapes. Figure 7 shows the local field potential and spiking activity time courses for a sample unit responding to a 45-Hz modulation rate of a strongly damped and a strongly ramped envelope shape. The recorded units expressed some variability in their specific phase delays, and normalised phase delays were thus calculated for each unit to account for this (for an analysis of the phase consistency/variability across units, see Supporting Information Fig. S2). To this end, the phase angle corresponding to the symmetrical envelope shape was subtracted (circular subtraction) from the two damped and the two ramped envelope shapes (for an analysis of non-normalised phase delays, see Supporting Information Fig. S3). Modulation of phase delays by envelope shapes was analysed by fitting a linear function to the normalised phase delays, separately for each unit and modulation rate. The estimated linear coefficient was used as the dependent measure.

For local field potentials, phase delays (angles) were systematically modulated for all modulation rates and both age groups (testing the linear coefficient against zero; for all $P_{FDR} < 0.001$, $r > 0.54$); phase delays for damped envelopes were leading (larger than zero) and phase angles for ramped envelopes were lagging (smaller than zero) compared to the symmetrical envelope (Fig. 8). Modulation of phase delays by envelope shapes was smaller for the 45-Hz modulation rate than the 128-Hz modulation rate (testing linear coefficients against each other; $P_{FDR} < 0.001$, $r > 0.6$) and the 256-Hz modulation rate ($P_{FDR} < 0.001$, $r = 0.264$). Modulation of phase delays was also larger for the 128-Hz modulation rate compared to the 256-Hz modulation rate ($P_{FDR} < 0.001$, $r = 0.433$). The phase delays for spike synchronisation showed a similar pattern (Fig. 8). Phase delays were systematically modulated for all modulation rates and both age groups (for all $P_{FDR} < 0.05$, $r > 0.3$) with the exception of the 256-Hz modulation rate for older rats ($P_{FDR} > 0.05$, $r = 0.216$). Modulation of phase delays did not significantly differ between modulation rates (for all $P_{FDR} > 0.05$, $r < 0.12$), although the phase delay patterns were very similar to the LFP phase delays (Fig. 8).

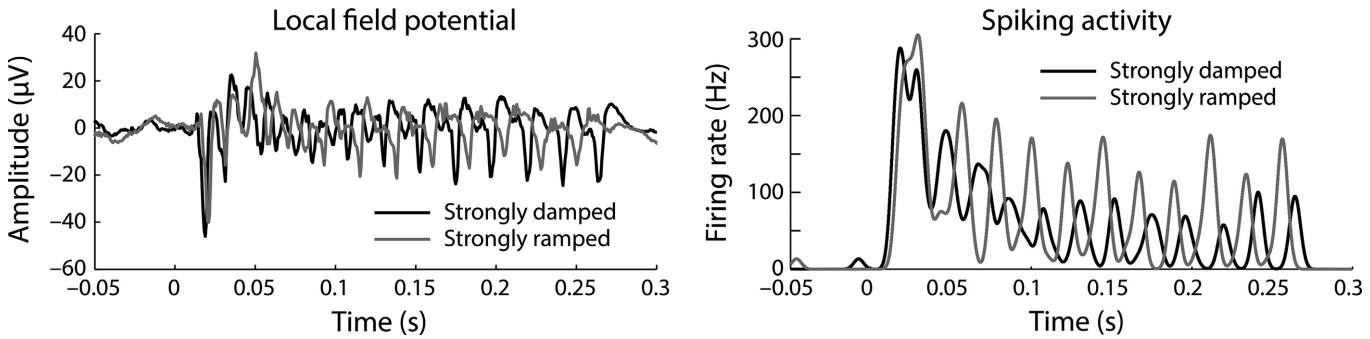

FIG. 7. Sample unit responses showing phase lag differences in neural synchronisation for different envelope shapes. Local field potentials (left) and spiking activity (right) for a strongly damped and a strongly ramped envelope shape for a 45-Hz modulation rate. Spiking activity time courses were calculated by convolving spikes with a Gaussian function (SD = 0.003 s).

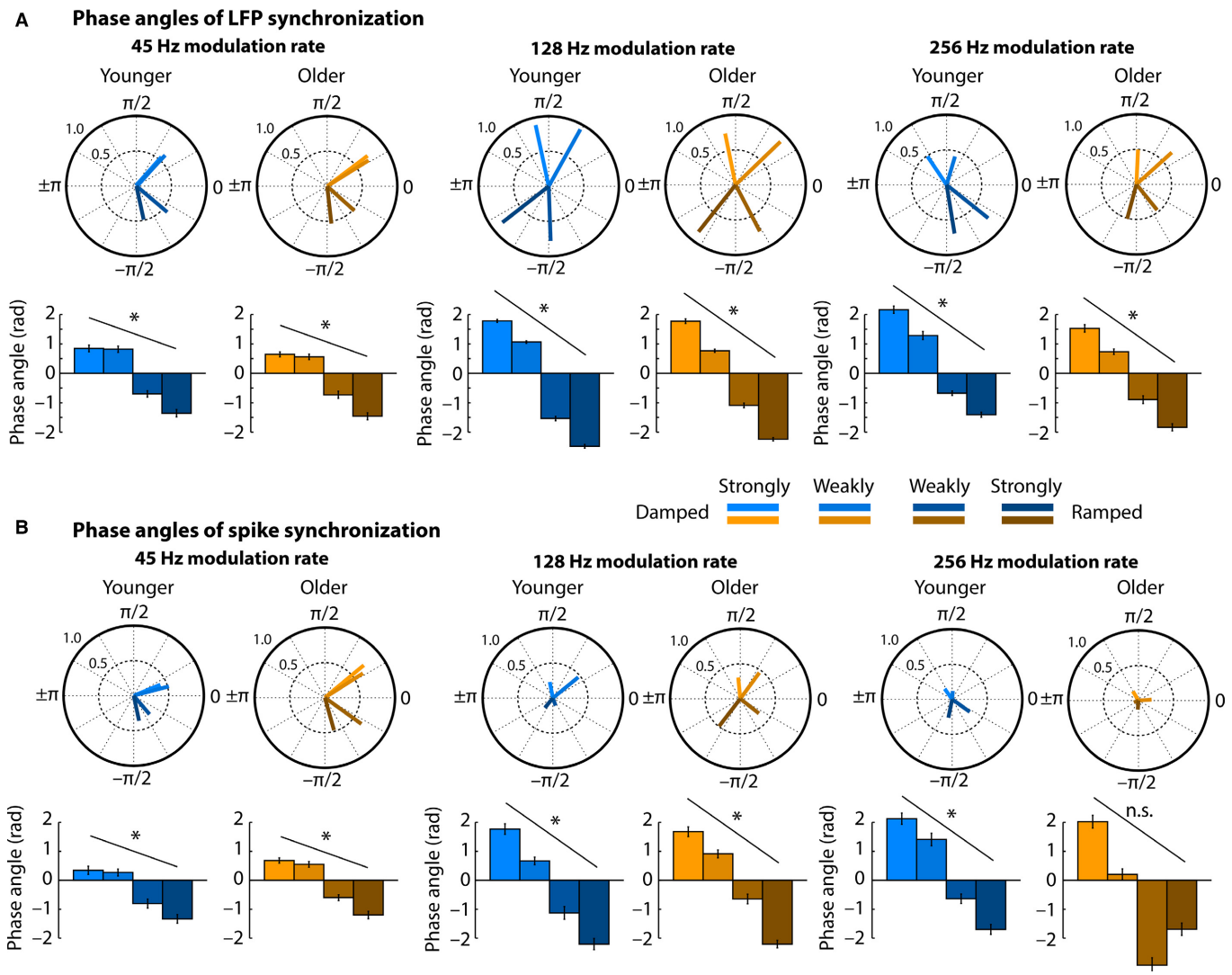

FIG. 8. Phase angles (delays) of local field potential and spike synchronisation. Circle plots show the resultant vector reflecting the phase angle consistency across units (i.e. a longer vector reflects higher consistency) and the mean phase angle. Phase angles of the four conditions (strongly damped, weakly damped, weakly ramped, strongly ramped) were normalised for each unit individually to their symmetrical condition (i.e. circular subtraction). Bar graphs show the mean phase angle and error bars reflect the circular standard error. Asterisks indicate a significant modulation of phase angles by envelope shapes. *$P_{FDR} < 0.05$, n.s., not significant. [Colour figure can be viewed at wileyonlinelibrary.com].

The degree to which phase delays were modulated by the envelope shapes appears to differ between modulation rate conditions; the 45-Hz modulation rate conditions seems less modulated, in particular for the two damped conditions. To obtain a better understanding of the relationship between the stimulus envelope shapes and the phase delays of neural synchronisation, we calculated hypothetical phase angles by thresholding the AM envelopes at 50, 65, and 80% stimulus level (Fig. 9).

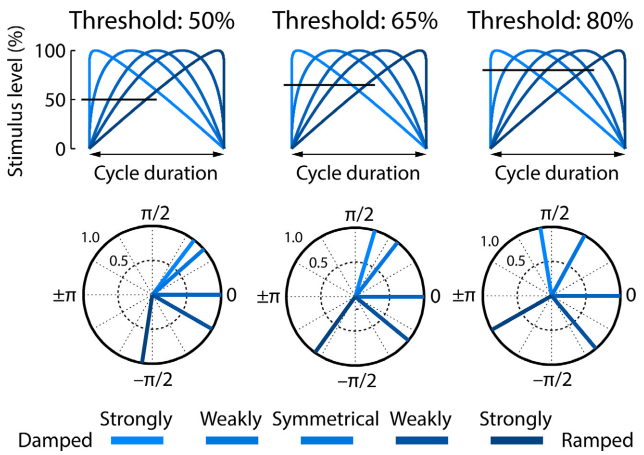

FIG. 9. Hypothetical relationship between stimulus envelope shape and synchronisation phase angle. The top row shows the five envelope shapes for one cycle. The horizontal line marks a hypothetical response threshold for three different example thresholds (50, 65, 80%). The bottom row reflect the phase angles (normalised to the symmetrical condition, similar to Fig. 8) corresponding to the point of threshold. [Colour figure can be viewed at wileyonlinelibrary.com].

From visual comparison between the phase angles displayed in Figs 8 and 9 it appears that neural synchronisation at 45-Hz modulation rates is associated with a lower response threshold (resemblance to 50% threshold), while 128- and 256-Hz modulation rates are associated with a higher response threshold (resemblance to 80% threshold; Fig. 9).

Discussion

This study investigated onset responses and neural synchronisation of LFP and spiking activity in the inferior colliculus of younger and older rats. We were specifically interested in the ability of neurons to encode both periodicity and envelope shape and the age-related changes from a neuron's synaptic activity to the spiking output. We observed a relative increase in sound onset-evoked neural activity from the LFP to spikes for older rats and a relative increase in neural synchronisation strength from LFPs to spikes for older rats for the 45-Hz modulation rate. Furthermore, neural synchronisation at fast modulation rates was reduced for older compared to younger rats.

Neural synchronisation to amplitude-modulated sounds

We observed clear peaks in the frequency spectrum in response to amplitude-modulated noises at 45, 128 and 256 Hz for LFPs and spikes (although spiking activity was not commonly synchronised with the 256-Hz modulation rate), with an overall decreasing synchronisation strength for higher modulation frequencies (Fig. 4). Our findings are consistent with previous studies on neural synchronisation in the inferior colliculus (Langner & Schreiner, 1988; Krishna & Semple, 2000; Palombi *et al.*, 2001; Walton *et al.*, 2002; Ter-Mikaelian *et al.*, 2007), which, however, exclusively focused on spiking activity. This study critically shows that neural synchronisation changes from LFP to spikes as evidenced by the different age-related patterns particularly at low modulation rates (i.e. 45 Hz; see below).

Neural synchronisation was not only affected by the modulation rate of the sounds but also in addition by the shape of the amplitude envelope. In particular, for the 45-Hz modulation rate, synchronisation strength was larger for damped compared to ramped envelope shapes for older rats, while the synchronisation strength was larger for ramped compared to damped shapes for younger rats (at least for the LFP; Fig. 6). The other intriguing finding was the quadratic trend observed for the 256-Hz modulation rate, such that neural activity synchronised more strongly with the damped and ramped envelope shapes than with the symmetrical envelope, and this quadratic trend was more pronounced in younger rats. Previous investigations of neural synchronisation to different envelope shapes have been sparse (Pressnitzer *et al.*, 2000; Lu *et al.*, 2001; Neuert *et al.*, 2001; Parthasarathy & Bartlett, 2011; for comparisons between click or noise burst sequences and amplitude-modulated sounds see Epping & Eggermont, 1986; Zheng & Escabi, 2013). One study focused on neural population responses measured at the scalp and observed larger neural synchronisation for damped than ramped envelope shapes for 128- and 256-Hz modulation rates (Parthasarathy & Bartlett, 2011). Others focused strongly on differences in firing rate magnitude between envelope shapes and only to some extent on synchronisation, observing, in contrast to this study (see Supporting Information Fig. S1), greater firing rates for ramped compared to damped envelope shapes (Pressnitzer *et al.*, 2000; Neuert *et al.*, 2001), although others have observed a more diverse pattern (Lu *et al.*, 2001). On the basis of the current data in combination with previous results, we suggest to remain cautious regarding functional interpretations of modulations in neural synchronisation strength or overall firing rates attributed to effects of envelope shape. Although there have only been a few studies investigating neural representations of envelope shapes (Pressnitzer *et al.*, 2000; Lu *et al.*, 2001; Neuert *et al.*, 2001; Parthasarathy & Bartlett, 2011), observations across studies showed considerable variability which, in our opinion, requires further research before clear conclusions are warranted.

We suggest that a more dominant coding scheme distinguishing between envelope shapes might be the timing or phase delay of neural synchronisation. We observed large changes in the phase delay of neural synchronisation for different envelope shapes (Fig. 8). For all modulation rates, synchronisation was systematically delayed (with respect to an AM cycle) from damped to ramped envelope shapes. However, for the 45-Hz modulation rate, almost no change in phase delay was observed between the strongly and weakly damped envelopes, but for all other envelope shapes (Fig. 8). A simple simulation (Fig. 9) suggests that the response threshold was lower for 45-Hz modulation rates than 128- and 256-Hz modulation rates. Critically, our results show that the phase delay (i.e. timing) of neural synchronisation represents envelope shapes at least up to 256 Hz, providing an important coding mechanism in addition to rate coding and coding by synchronisation strength which have previously been emphasised (Epping & Eggermont, 1986; Pressnitzer *et al.*, 2000; Lu *et al.*, 2001; Walton *et al.*, 2002; Gao & Wehr, 2015; for an emphasis on spike timing precision see also Zheng & Escabí, 2008; Zheng & Escabi, 2013). The observed timing differences in neural synchronisation might be important to perceptually distinguish (potentially superimposed) sounds that exhibit different envelope shapes. Yet, the timing differences observed here are likely inherited from neural circuitries preceding the inferior colliculus within the auditory pathway as suggested by the absence of phase delay changes as a function of envelope shapes in LFP-spike synchronisation (see Supporting Information Figs S4 and S5).

Effects of ageing on response magnitude and neural synchronisation strength

This study aimed to investigate the age-related changes of neural signal transduction from the synaptic (input; LFP) activity to spiking

output. We observed a relative increase in sound onset-evoked neural activity from the LFP to spikes for older rats (Fig. 2) and a relative increase in neural synchronisation strength from LFPs to spikes for older rats at 45-Hz modulation rates, whereas synchronisation strength was reduced for 256-Hz modulation rates (Fig. 4).

Previous work in animals showed enhanced firing rates along the ascending auditory pathway following hearing loss and accompanying ageing (Popelár *et al.*, 1987; Syka *et al.*, 1994; Hughes *et al.*, 2010; Manzoor *et al.*, 2012). In particular, auditory cortex neural activity appears to be enhanced in animals with hearing loss (Stolzberg *et al.*, 2012) as well as in aged animals and humans (Laffont *et al.*, 1989; Hughes *et al.*, 2010; Herrmann *et al.*, 2013b, 2016; Bidelman *et al.*, 2014). Assuming that synaptic neuronal activity at the soma and dendrites (input to a neuron or neuronal population) strongly contributes to the LFP and spiking reflects the output of a neuron or neuronal population (Bullock, 1997; Logothetis *et al.*, 2001; Logothetis & Wandell, 2004; Buzsáki *et al.*, 2012), the current data show that within a single midbrain structure (inferior colliculus) neuronal response magnitudes become relatively enhanced from synaptic to spiking activity in aged animals.

Previous studies investigating spike synchronisation in ageing animals reported that temporal modulation transfer functions shift from a band-pass to a low-pass shape (Palombi *et al.*, 2001; Schatteman *et al.*, 2008). That is, synchronisation strength increases at slower modulation rates and decreases at faster modulation rates in older animals. Consistently, the current data reveal an age-related increase in spike synchronisation at a slow modulation rate (45 Hz) and a decrease in LFP and spike synchronisation at faster modulation rates (128 and 256 Hz; although not statistically significant in some cases). Scalp recordings in humans and animals have shown similar age-related increases in neural synchronisation for slower modulation rates (Boettcher *et al.*, 2002; Purcell *et al.*, 2004) and a decrease in synchronisation strength for fast stimulus modulation rates (Grose *et al.*, 2009; Clinard *et al.*, 2010; Anderson *et al.*, 2012; Parthasarathy & Bartlett, 2012; Bidelman *et al.*, 2014; Parthasarathy *et al.*, 2014), although in particular responses to slow rates may also have significant contributions from auditory cortex in such scalp recordings (Herdman *et al.*, 2002; Coffey *et al.*, 2016).

In particular, our LFP synchronisation data critically add to the existing body of work: (i) The data show that neural activity within the ageing inferior colliculus synchronises with the fast temporal modulation of sounds (at least up to 256 Hz), precisely capturing different stimulus envelope shapes in the neural phase delay. (ii) We show that neural synchronisation to a slow modulation rate (here 45 Hz) relatively increases from the synaptic activity (LFP) to spiking output in older animals. That is, no age difference in neural synchronisation was observed for the LFPs. In contrast, neurons in the aged inferior colliculus elicited precisely phase-locked bursts of spikes, whereas in younger animals spikes were more distributed over an AM cycle and thus less synchronised (see Figs 4 and 5). (iii) Neural synchronisation strength decreased from damped to ramped envelope shapes (45-Hz modulation rate, LFP) for older rats whereas it increased in younger rats. (iv) Synchronisation strength in older animals was reduced for modulation rates greater than 100 Hz.

One of the most consistent changes within the central auditory system following hearing loss and accompanying ageing is the reduction in neural inhibition along the ascending auditory pathway (Raza *et al.*, 1994; Caspary *et al.*, 1995, 2008; Vale *et al.*, 2004; Burianova *et al.*, 2009; Takesian *et al.*, 2009, 2012; Llano *et al.*, 2012; Rabang *et al.*, 2012; Gao *et al.*, 2015). Accordingly, recent observations of enhanced neural responses (excitability) due to hearing loss and ageing have been discussed in the context of reduced neural inhibition (Hughes *et al.*, 2010; Herrmann *et al.*, 2016). Neural inhibition modulates sound-evoked neural activity levels (Faingold *et al.*, 1989; Pollak & Park, 1993), which is consistent with our observation of a relatively enhanced onset response from LFP to spiking activity and reduced N1 latencies for older compared to younger rats (Figs 2 and 3).

Neural inhibition has also been shown to be crucial for shaping neural activity elicited by amplitude-modulated sounds (Yang & Pollak, 1997; Backoff *et al.*, 1999; Cai & Caspary, 2015; but see also Caspary *et al.*, 2002; Zhang & Kelly, 2003). Yet, the direction in which a reduction in neural inhibition affects neural synchronisation is not clear. For example, reduced neural inhibition in the cochlear nucleus led to decreased neural synchronisation to amplitude-modulated sounds (Backoff *et al.*, 1999). A different study shows for neurons in the lateral lemniscus that a reduction in neural inhibition leads to an increase in synchronisation strength for neurons that did not synchronise strongly before blockage of neural inhibition and to a decrease in synchronisation strength for neurons that strongly synchronised before the blockage of inhibition (Yang & Pollak, 1997). In the inferior colliculus, synchronisation was mostly unaffected by reduced inhibition (Caspary *et al.*, 2002). These differences are in line with computational modelling suggesting that the influence of neural inhibition on neural synchronisation is rather complex (Rabang *et al.*, 2012).

A tentative interpretation of the current findings is that the age-related increase in synchronisation strength for the low modulation frequency (45 Hz) and the age-related decrease in synchronisation strength for the high modulation frequency (e.g. 256 Hz) are both the result of a reduction in neural inhibition in the auditory system of ageing rats. Although there are other potential mechanisms, such as changes in ion channel (K, Cl, HCN) distribution, changes in short-term plasticity or changes in excitatory receptors (Kotak *et al.*, 2005), reduction in inhibition is well supported by prior studies (Caspary *et al.*, 2008; Rabang *et al.*, 2012) and could potentially show modulation-frequency dependent changes in net excitability. Reduced neural inhibition leads to increased firing rates (assuming no concurrent decreases in excitation) which in turn might lead to a larger modulation of firing rate induced by the amplitude modulation, that is, increased synchronisation strength. Another possibility is that an age-related reduction in neural inhibition is accompanied by reduced excitation, similar to hearing loss during development (Kotak & Sanes, 1997; Vale & Sanes, 2002). This would lead to unchanged or decreased firing rates, but might still lead to increased synchronisation strength because the net excitation becomes restricted to near the peak phase of the AM cycle. Critically, reduced neural inhibition might also result in an increase in the amount of temporal jitter (by changing the excitation-inhibition balance) either within the input from a single neuron or across inputs from multiple neurons, potentially reducing temporal selectivity (Wehr & Zador, 2003; Isaacson & Scanziani, 2011). For low modulation rates, a mild increase in jitter could be offset by a relative increase in firing rate. In contrast, a mild increase in temporal jitter would decrease neural synchronisation for high modulation rates because the duration of an AM cycle would likely be comparable to or shorter than the jitter. In addition, the input rate and/or synaptic depression might systematically vary depending on the AM rate of the stimulus (Joris *et al.*, 2004; Rabang & Bartlett, 2011). For example, if the input rate were to decrease or synaptic depression to increase with AM rate, this would likely lead to inputs near or below the threshold for high AM rates (even with reduced inhibition) and thus to a reduction in synchronisation strength as assessed by spiking activity. Future studies combing empirical and

computation approaches are needed to shed more light on the role of the excitation-inhibition balance in age-related changes in neural synchronisation. Furthermore, additional work is necessary to explore other mechanisms for increasing neuronal excitability, such as mechanisms that alter resting membrane potential, input resistance or time constants.

Conclusions

This study investigated the age-related changes in neural response magnitudes and neural synchronisation in inferior colliculus neurons focusing on local field potentials and spiking. Activity in the inferior colliculus allows distinguishing stimulus envelope shapes for modulation rates higher than 250 Hz. Ageing was accompanied by a relative increase in response magnitude to sound onsets and a relative increase in neural synchronisation strength from the local field potential (synaptic activity) to spiking output for older rats. Ageing was also associated with decreased neural synchronisation strength at higher amplitude-modulation rates. The current data show that signal transformation within a single midbrain structure (inferior colliculus) is altered in aged animals.

Disclosure

The authors claim no actual or potential conflicts of interest.

Author contributions

BH analysed data and drafted the manuscript. AP designed the study, collected data and drafted the manuscript. ELB designed the study, collected data and drafted the manuscript.

Data accessibility

The article's data are available on the dryad data repository (https://datadryad.org/).

Supporting Information

Additional supporting information can be found in the online version of this article:

Appendix S1. Methods and results.

Figure S1. Normalised firing rate difference between damped vs. ramped conditions in the sustained period 0.05–0.275 s.

Figure S2. Phase consistency of LFP neural synchronisation across units.

Figure S3. Absolute phase delay (angle) for age groups and modulation rates.

Figure S4. LFP-spike synchronisation strength.

Figure S5. Phase delays (angle) of LFP-spike synchronisation.

Acknowledgements

This study was supported by NIDCD DC-011580 to ELB and the Brain and Mind Institute at the University of Western Ontario (postdoctoral fellowship award to BH).

References

Adams, J. (1979) Ascending projections to the inferior colliculus. *J. Comp. Neurol.*, **183**, 519–538.

Akeroyd, M.A. & Patterson, R.D. (1995) Discrimination of wideband noises modulated by a temporally asymmetric function. *J. Acoust. Soc. Am.*, **98**, 2466–2474.

Anderson, S., Parbery-Clark, A., White-Schwoch, T. & Kraus, N. (2012) Aging affects neural precision of speech encoding. *J. Neurosci.*, **32**, 14156–14164.

Backoff, P.M., Palombi, P.S. & Caspary, D.M. (1999) γ-Aminobutyric acidergic and glycinergic inputs shape coding of amplitude modulation in the chinchilla cochlear nucleus. *Hear. Res.*, **134**, 77–88.

Barsz, K., Ison, J.R., Snell, K.B. & Walton, J.P. (2002) Behavioral and neural measures of auditory temporal acuity in aging humans and mice. *Neurobiol. Aging*, **23**, 565–578.

Bartlett, E.L. & Wang, X. (2005) Long-lasting modulation by stimulus context in primate auditory cortex. *J. Neurophysiol.*, **94**, 83–104.

Bartlett, E.L. & Wang, X. (2007) Neural representations of temporally modulated signals in the auditory thalamus of awake primates. *J. Neurophysiol.*, **97**, 1005–1017.

Bartlett, E.L. & Wang, X. (2011) Correlation of neural response properties with auditory thalamus subdivisions in the awake marmoset. *J. Neurophysiol.*, **105**, 2647–2667.

Belitski, A., Panzeri, S., Magri, C., Logothetis, N.K. & Kayser, C. (2010) Sensory information in local field potentials and spikes from visual and auditory cortices: time scales and frequency bands. *J. Comput. Neurosci.*, **29**, 533–545.

Benjamini, Y. & Hochberg, Y. (1995) Controlling the false discovery rate: a practical and powerful approach to multiple testing. *J. Roy. Stat. Soc. Ser. B*, **57**, 289–300.

Bibikov, N.G. (2002) Coding of amplitude-modulated signals in the cochlear nucleus of a grass frog. *Acoust. Phys.*, **48**, 388–399.

Bidelman, G.M., Villafuerte, J.W., Moreno, S. & Alain, C. (2014) Age-related changes in the subcorticalecortical encoding and categorical perception of speech. *Neurobiol. Aging*, **35**, 2526–2540.

Boettcher, F.A., Poth, E.A., Mills, J.H. & Dubno, J.R. (2001) The amplitude-modulation following response in young and aged human subjects. *Hear. Res.*, **153**, 32–42.

Boettcher, F.A., Madhotra, D., Poth, E.A. & Mills, J.H. (2002) The frequency-modulation following response in young and aged human subjects. *Hear. Res.*, **165**, 10–18.

Bullock, T.H. (1997) Signals and signs in the nervous system: the dynamic anatomy of electrical activity is probably information-rich. *Proc. Natl Acad. Sci.*, **94**, 1–6.

Burianova, J., Ouda, L., Profant, O. & Syka, J. (2009) Age-related changes in GAD levels in the central auditory system of the rat. *Exp. Gerontol.*, **44**, 161–169.

Buzsáki, G., Anastassiou, C.A. & Koch, C. (2012) The origin of extracellular fields and currents – EEG, ECoG, LFP and spikes. *Nat. Rev. Neurosci.*, **13**, 407–420.

Cai, R. & Caspary, D.M. (2015) GABAergic inhibition shapes SAM responses in rat auditory thalamus. *Neuroscience*, **299**, 146–155.

Canlon, B., Illing, R.B. & Walton, J.P. (2010). Cell biology and physiology of the aging central auditory pathway. In Gordon-Salant, S., Frisina, R.D., Popper, A.N. & Fay, R.R. (Eds), *The Aging Auditory System*. Springer, New York, pp. 39–74.

Caspary, D.M., Milbrandt, J.C. & Helfert, R.H. (1995) Central auditory aging: GABA changes in the inferior colliculus. *Exp. Gerontol.*, **30**, 349–360.

Caspary, D.M., Palombi, P.S. & Hughes, L.F. (2002) GABAergic inputs shape responses to amplitude modulated stimuli in the inferior colliculus. *Hear. Res.*, **168**, 163–173.

Caspary, D.M., Ling, L., Turner, J.G. & Hughes, L.F. (2008) Inhibitory neurotransmission, plasticity and aging in the mammalian central auditory system. *J. Exp. Biol.*, **211**, 1781–1791.

Clinard, C.G., Tremblay, K.L. & Krishnan, A.R. (2010) Aging alters the perception and physiological representation of frequency: evidence from human frequency-following response recordings. *Hear. Res.*, **264**, 48–55.

Coffey, E.B.J., Herholz, S.C., Chepesiuk, A.M.P., Baillet, S. & Zatorre, R.J. (2016) Cortical contributions to the auditory frequency-following response revealed by MEG. *Nat. Commun.*, **7**, 11070.

Drummond, G.B. (2009) Reporting ethical matters in The Journal of Physiology: standards and advice. *J. Physiol.*, **587**, 713–719.

Epping, W.J.M. & Eggermont, J.J. (1986) Sensitivity of neurons in the auditory midbrain of the grassfrog to temporal characteristics of sound. II. Stimulation with amplitude modulated sound. *Hear. Res.*, **24**, 55–72.

Faingold, C.L., Gehlbach, G. & Caspary, D.M. (1989) On the role of GABA as an inhibitory neurotransmitter in inferior colliculus neurons: iontophoretic studies. *Brain Res.*, **500**, 302–312.
Furukawa, S. & Moore, B.C.J. (1997) Effect of the relative phase of amplitude modulation on the detection of modulation on two carriers. *J. Acoust. Soc. Am.*, **102**, 3657–3664.
Gao, X. & Wehr, M. (2015) A coding transformation for temporally structured sounds within auditory cortical neurons. *Neuron*, **86**, 1–12.
Gao, F., Wang, G., Ma, W., Ren, F., Li, M., Dong, Y., Liu, C., Liu, B. *et al.* (2015) Decreased auditory GABA+ concentrations in presbycusis demonstrated by edited magnetic resonance spectroscopy. *NeuroImage*, **106**, 311–316.
Gardner, M.J. & Altman, D.G. (1986) Confidence intervals rather than P values: estimation rather than hypothesis testing. *Stat. Med.*, **292**, 746–750.
Genovese, C.R., Lazar, N.A. & Nichols, T. (2002) Thresholding of statistical maps in functional neuroimaging using the false discovery rate. *NeuroImage*, **15**, 870–878.
Gourévitch, B. & Edeline, J.-M. (2011) Age-related changes in the guinea pig auditory cortex: relationship with brainstem changes and comparison with tone-induced hearing loss. *Eur. J. Neurosci.*, **34**, 1953–1965.
Grose, J.H., Mamo, S.K. & Hall, J.W. III (2009) Age effects in temporal envelope processing: speech unmasking and auditory steady state responses. *Ear Hear.*, **30**, 568–575.
Haegens, S., Nácher, V., Luna, R., Romo, R. & Jensen, O. (2011) α-Oscillations in the monkey sensorimotor network influence discrimination performance by rhythmical inhibition of neuronal spiking. *Proc. Natl Acad. Sci.*, **108**, 19377–19382.
Heil, P. (2004) First-spike latency of auditory neurons revisited. *Curr. Opin. Neurobiol.*, **14**, 461–647.
Herdman, A.T., Lins, O., Van Roon, P., Stapells, D.R., Scherg, M. & Picton, T.W. (2002) Intracerebral sources of human auditory steady-state responses. *Brain Topogr.*, **15**, 69–86.
Herrmann, B., Henry, M.J., Grigutsch, M. & Obleser, J. (2013a) Oscillatory phase dynamics in neural entrainment underpin illusory percepts of time. *J. Neurosci.*, **33**, 15799–15809.
Herrmann, B., Henry, M.J., Scharinger, M. & Obleser, J. (2013b) Auditory filter width affects response magnitude but not frequency specificity in auditory cortex. *Hear. Res.*, **304**, 128–136.
Herrmann, B., Parthasarathy, A., Han, E.X., Obleser, J. & Bartlett, E.L. (2015) Sensitivity of rat inferior colliculus neurons to frequency distributions. *J. Neurophysiol.*, **114**, 2941–2954.
Herrmann, B., Henry, M.J., Johnsrude, I.S. & Obleser, J. (2016) Altered temporal dynamics of neural adaptation in the aging human auditory cortex. *Neurobiol. Aging*, **45**, 10–22.
Hughes, L.F., Turner, J.G., Parrish, J.L. & Caspary, D.M. (2010) Processing of broadband stimuli across A1 layers in young and aged rats. *Hear. Res.*, **264**, 79–85.
Irino, T. & Patterson, R.D. (1996) Temporal asymmetry in the auditory system. *J. Acoust. Soc. Am.*, **99**, 2316–2331.
Isaacson, J.S. & Scanziani, M. (2011) How inhibition shapes cortical activity. *Neuron*, **72**, 231–243.
Joris, P.X. & Yin, T.C. (1992) Responses to amplitude-modulated tones in the auditory nerve of the cat. *J. Acoust. Soc. Am.*, **91**, 215–232.
Joris, P.X., Schreiner, C.E. & Rees, A. (2004) Neural processing of amplitude-modulated sounds. *Physiol. Rev.*, **84**, 541–577.
Kadner, A. & Berrebi, A.S. (2008) Encoding of temporal features of auditory stimuli in the medial nucleus of the trapezoid body and superior paraolivary nucleus of the rat. *Neuroscience*, **151**, 868–887.
Kajikawa, Y. & Schroeder, C.E. (2011) How local is the local field potential? *Neuron*, **72**, 847–858.
Kale, S. & Heinz, M.G. (2010) Envelope coding in auditory nerve fibers following noise-induced hearing loss. *J. Assoc. Res. Otolaryngol.*, **11**, 657–673.
Kayser, C., Wilson, C., Safaai, H., Sakata, S. & Panzeri, S. (2015) Rhythmic auditory cortex activity at multiple timescales shapes stimulus-response gain and background firing. *J. Neurosci.*, **35**, 7750–7762.
Kotak, V.C. & Sanes, D.H. (1997) Deafferentation weakens excitatory synapses in the developing central auditory system. *Eur. J. Neurosci.*, **9**, 2340–2347.
Kotak, V.C., Fujisawa, S., Lee, F.A., Karthikeyan, O., Aoki, C. & Sanes, D.H. (2005) Hearing loss raises excitability in the auditory cortex. *J. Neurosci.*, **25**, 3908–3918.
Krishna, B.S. & Semple, M.N. (2000) Auditory temporal processing: responses to sinusoidally amplitude-modulated tones in the inferior colliculus. *J. Neurophysiol.*, **84**, 255–273.
Lachaux, J.-P., Rodriguez, E., Martinerie, J. & Varela, F.J. (1999) Measuring phase synchrony in brain signals. *Hum. Brain Mapp.*, **8**, 194–208.
Laffont, F., Bruneau, N., Roux, S., Agar, N., Minz, M. & Cathala, H.P. (1989) Effects of age on auditory evoked responses (AER) and augmenting-reducing. *Clin. Neurophysiol.*, **19**, 15–23.
Lakatos, P., Karmos, G., Mehta, A.D., Ulbert, I. & Schroeder, C.E. (2008) Entrainment of neuronal oscillations as a mechanism of attentional selection. *Science*, **320**, 110–113.
Langner, G. & Schreiner, C.E. (1988) Periodicity coding in the inferior colliculus of the cat. Neuronal mechanisms. *J. Neurophysiol.*, **60**, 1799–1822.
Lee, C.C. & Sherman, S.M. (2010) Drivers and modulators in the central auditory pathways. *Front. Neurosci.*, **4**, 79–86.
Llano, D.A., Turner, J. & Caspary, D.M. (2012) Diminished cortical inhibition in an aging mouse model of chronic tinnitus. *J. Neurosci.*, **32**, 16141–16148.
Logothetis, N.K. & Wandell, B.A. (2004) Interpreting the BOLD signal. *Annu. Rev. Physiol.*, **66**, 735–769.
Logothetis, N.K., Pauls, J., Augath, M., Trinath, T. & Oettermann, A. (2001) Neurophysiological investigation of the basis of the fMRI signal. *Nature*, **412**, 150–157.
Lu, T., Liang, L. & Wang, X. (2001) Temporal and rate representations of time-varying signals in the auditory cortex of awake primates. *Nat. Neurosci.*, **4**, 1131–1138.
Malone, B.J., Scott, B.H. & Semple, M.N. (2007) Dynamic amplitude coding in the auditory cortex of awake rhesus macaques. *J. Neurophysiol.*, **98**, 1451–1474.
Manzoor, N.F., Licari, F.G., Klapchar, M., Elkin, R.L., Gao, Y., Chen, G. & Kaltenbach, J.A. (2012) Noise-induced hyperactivity in the inferior colliculus: its relationship with hyperactivity in the dorsal cochlear nucleus. *J. Neurophysiol.*, **108**, 976–988.
Milbrandt, J.C., Albin, R.L. & Caspary, D.M. (1994) Age-related decrease in GABAB receptor binding in the Fischer 344 rat inferior colliculus. *Neurobiol. Aging*, **15**, 699–703.
Moore, B.C.J. & Skrodzka, E. (2002) Detection of frequency modulation by hearing-impaired listeners: effects of carrier frequency, modulation rate, and added amplitude modulation. *J. Acoust. Soc. Am.*, **111**, 327–335.
Neuert, V., Pressnitzer, D., Patterson, R.D. & Winter, I.M. (2001) The responses of single units in the inferior colliculus of the guinea pig to damped and ramped sinusoids. *Hear. Res.*, **159**, 36–52.
Palombi, P.S., Backoff, P.M. & Caspary, D.M. (2001) Responses of young and aged rat inferior colliculus neurons to sinusoidally amplitude modulated stimuli. *Hear. Res.*, **153**, 174–180.
Parthasarathy, A. & Bartlett, E.L. (2011) Age-related auditory deficits in temporal processing in F-344 rats. *Neuroscience*, **192**, 619–630.
Parthasarathy, A. & Bartlett, E.L. (2012) Two-channel recording of auditory-evoked potentials to detect age-related deficits in temporal processing. *Hear. Res.*, **289**, 52–62.
Parthasarathy, A., Datta, J., Torres, J.A.L., Hopkins, C. & Bartlett, E.L. (2014) Age-related changes in the relationship between auditory brainstem responses and envelope-following responses. *J. Assoc. Res. Otolaryngol.*, **15**, 649–661.
Patterson, R.D. (1994) The sound of a sinusoid: spectral models. *J. Acoust. Soc. Am.*, **96**, 1409–1418.
Paxinos, G. & Watson, C. (2006) *The Rat Brain in Stereotaxic Coordinates*. Academic Press, New York.
Pichora-Fuller, M.K. (2003) Processing speed and timing in aging adults: psychoacoustics, speech perception, and comprehension. *Int. J. Audiol.*, **42**, S59–S67.
Picton, T.W., John, S.M., Dimitrijevic, A. & Purcell, D.W. (2003) Human auditory steady-state responses. *Int. J. Audiol.*, **42**, 177–219.
Pollak, G.D. & Park, T.J. (1993) The effects of GABAergic inhibition on monaural response properties of neurons in the mustache bat's inferior colliculus. *Hear. Res.*, **65**, 99–117.
Pollak, G.D., Burger, R.M. & Klug, A. (2003) Dissecting the circuitry of the auditory system. *Trends Neurosci.*, **26**, 33–39.
Popelár, J., Syka, J. & Berndt, H. (1987) Effect of noise on auditory evoked responses in awake guinea pigs. *Hear. Res.*, **26**, 239–247.
Pressnitzer, D., Winter, I.M. & Patterson, R.D. (2000) The responses of single units in the ventral cochlear nucleus of the guinea pig to damped and ramped sinusoids. *Hear. Res.*, **149**, 155–166.
Preuß, A. & Müller-Preuss, P. (1990) Processing of amplitude modulated sounds in the medial geniculate body of squirrel monkeys. *Exp. Brain Res.*, **79**, 207–211.

Purcell, D.W., John, S.M., Schneider, B.A. & Picton, T.W. (2004) Human temporal auditory acuity as assessed by envelope following responses. *J. Acoust. Soc. Am.*, **116**, 3581–3593.

Rabang, C.F. & Bartlett, E.L. (2011) A computational model of cellular mechanisms of temporal coding in the medial geniculate body (MGB). *PLoS One*, **6**, e29375.

Rabang, C.F., Parthasarathy, A., Venkataraman, Y., Fisher, Z.L., Gardner, S.M. & Bartlett, E.L. (2012) A computational model of inferior colliculus responses to amplitude modulated sounds in young and aged rats. *Front. Neural Circuits*, **6**, 77.

Raza, A., Milbrandt, J.C., Arneric, S.P. & Caspary, D.M. (1994) Age-related changes in brainstem auditory neurotransmitters: measures of GABA and acetylcholine function. *Hear. Res.*, **77**, 221–230.

Rosenthal, R. & Rubin, D.B. (2003) r equivalent: a simple effect size indicator. *Psychol. Methods*, **8**, 492–496.

Schatteman, T.A., Hughes, L.F. & Caspary, D.M. (2008) Age-related loss of temporal processing: altered responses to amplitude modulated tones in rat dorsal cochlear nucleus. *Neuroscience*, **154**, 329–337.

Schneider, B.A., Pichora-Fuller, M.K., Kowalchuk, D. & Lamb, M. (1994) Gap detection and the precedence effect in young and old adults. *J. Acoust. Soc. Am.*, **95**, 980–991.

Schvartz, K.C. & Chatterjee, M. (2012) Gender identification in younger and older adults: use of spectral and temporal cues in noise-vocoded speech. *Ear Hear.*, **33**, 411–420.

Stolzberg, D., Chrostowski, M., Salvi, R.J. & Allman, B. (2012) Intracortical circuits amplify sound-evoked activity in primary auditory cortex following systemic injection of salicylate in the rat. *J. Neurophysiol.*, **108**, 200–214.

Syka, J. (2010) The Fischer 344 rat as a model of presbycusis. *Hear. Res.*, **264**, 70–78.

Syka, J., Rybalko, N. & Popelár, J. (1994) Enhancement of the auditory cortex evoked responses in awake guinea pigs after noise exposure. *Hear. Res.*, **78**, 158–168.

Takesian, A.E., Kotak, V.C. & Sanes, D.H. (2009) Developmental hearing loss disrupts synaptic inhibition: implications for auditory processing. *Future Neurol.*, **4**, 331–349.

Takesian, A.E., Kotak, V.C. & Sanes, D.H. (2012) Age-dependent effect of hearing loss on cortical inhibitory synapse function. *J. Neurophysiol.*, **107**, 937–947.

Ter-Mikaelian, M., Sanes, D.H. & Semple, M.N. (2007) Transformation of temporal properties between auditory midbrain and cortex in the awake Mongolian gerbil. *J. Neurosci.*, **27**, 6091–6102.

Vale, C. & Sanes, D.H. (2002) The effect of bilateral deafness on excitatory and inhibitory synaptic strength in the inferior colliculus. *Eur. J. Neurosci.*, **16**, 2394–2404.

Vale, C., Juiz, J.M., Moore, D.R. & Sanes, D.H. (2004) Unilateral cochlear ablation produces greater loss of inhibition in the contralateral inferior colliculus. *Eur. J. Neurosci.*, **20**, 2133–2140.

Vernier, V.G. & Galambos, R. (1957) Response of single medial geniculate units to repetitive click stimuli. *Am. J. Physiol.*, **188**, 233–237.

Walton, J.P. (2010) Timing is everything: temporal processing deficits in the aged auditory brainstem. *Hear. Res.*, **264**, 63–69.

Walton, J.P., Simon, H. & Frisina, R.D. (2002) Age-related alterations in the neural coding of envelope periodicities. *J. Neurophysiol.*, **88**, 565–578.

Wayne, R.V. & Johnsrude, I.S. (2015) A review of causal mechanisms underlying the link between age-related hearing loss and cognitive decline. *Ageing Res. Rev.*, **23**, 154–166.

Wehr, M. & Zador, A.M. (2003) Balanced inhibition underlies tuning and sharpens spike timing in auditory cortex. *Nature*, **426**, 442–446.

Whittingstall, K. & Logothetis, N.K. (2009) Frequency-band coupling in surface EEG reflects spiking activity in monkey visual cortex. *Neuron*, **64**, 281–289.

Yang, L. & Pollak, G.D. (1997) Differential response properties to amplitude modulated signals in the dorsal nucleus of the lateral lemniscus of the mustache bat and the roles of GABAergic inhibition. *J. Neurophysiol.*, **77**, 324–340.

Zhang, H. & Kelly, J.B. (2003) Glutamatergic and GABAergic regulation of neural responses in inferior colliculus to amplitude-modulated sounds. *J. Neurophysiol.*, **90**, 477–490.

Zheng, Y. & Escabi, M.A. (2013) Proportional spike-timing precision and firing reliability underlie efficient temporal processing of periodicity and envelope shape cues. *J. Neurophysiol.*, **110**, 587–606.

Zheng, Y. & Escabí, M.A. (2008) Distinct roles for onset and sustained activity in the neuronal code for temporal periodicity and acoustic envelope shape. *J. Neurosci.*, **28**, 14230–14244.